Effects of velocity-dependent and spin-orbit terms of the Skyrme interaction on neutron elastic scattering observables

N. Hoang Tung [1,2,3,4,*] D. Quang Tam,[5,6,†] Vinh N. T. Pham [7] Chi Lam Truong,[8,‡] and T. V. Nhan Hao [5,9]

[1]*Institute of Fundamental and Applied Sciences, Duy Tan University, Ho Chi Minh City 700000, Vietnam*
[2]*Faculty of Natural Science, Duy Tan University, Da Nang City 550000, Vietnam*
[3]*Department of Nuclear Physics and Nuclear Engineering, Faculty of Physics and Engineering Physics,*
University of Science, Ho Chi Minh City 700000, Vietnam
[4]*Vietnam National University, Ho Chi Minh City 700000, Vietnam*
[5]*Faculty of Physics, University of Education, Hue University, Hue City 52000, Vietnam*
[6]*Faculty of Basic Sciences, University of Medicine and Pharmacy, Hue University, Hue City 52000, Vietnam*
[7]*Ho Chi Minh City University of Education, Ho Chi Minh City 700000, Vietnam*
[8]*NTT Hi-Tech Institute, Nguyen Tat Thanh University, Ho Chi Minh City 700000, Vietnam*
[9]*Center for Theoretical and Computational Physics, University of Education, Hue University, Hue City 52000, Vietnam*

Elastic scattering of a series of doubly closed-shell nuclei at low energy has been described in the framework of optical potential model generated from the particle-vibration coupling approach on top of the collective excited states obtained from the random-phase approximation. We focus on the effects of the spin-orbit and velocity-dependent interaction on the angular distributions and analyzing powers by comparing these observables with experimental data. It has been found that the contribution of the two-body velocity-dependent and two-body spin-orbit terms are important to improve results for ^{16}O, ^{40}Ca, ^{48}Ca, and ^{208}Pb. The velocity-dependent interactions strongly reduce the absorption on the surface while the spin-orbit interactions sightly increase the absorption in the interior.

I. INTRODUCTION

Microscopic optical potential model is expected to be a reliable and predictable tool for nuclear reaction calculations in the region of exotic nuclei [1,2]. To generate the microscopic optical potential at low energy ($E < 50$ MeV) where the specific nuclear structure effects become important, the *ab initio* methods and nuclear structure models are promising approaches since they can link directly the underlying nucleon-nucleon (NN) interaction to nucleon-nucleus (NA) scattering observables. Although there has been impressive progress over the past few years, the recent *ab initio* calculations (using the bare NN interaction) are still limited in the light and medium regions [3–7]. Recently, the nuclear many-body approaches [Hartree-Fock-Bogoliubov (HFB), Hartree-Fock plus Bardeen–Cooper–Schrieffer (HF + BCS), and (Quasiparticle) random phase approximation [(Q)RPA)]] [8–15] based on self-consistent mean-field using the effective phenomenological NN interaction (which breaks the explicit link with the bare NN interaction) have proven their ability

to describe globally a wide range of nuclear structure observables. This is a cornerstone for the so-called nuclear structure models (NSM) could be used to build the microscopic optical potential for nucleon elastic scattering by the light-, medium-, and heavy-nuclei regions [16–23]. Let us show, for example, the standard form of the widely used effective Skyrme interaction between two nucleons with space, spin, and isospin variables $\mathbf{r}_i$, σ_i, and τ_i:

$$V_{\text{Skyrme}}(\mathbf{r}_1, \mathbf{r}_2) = t_0(1 + x_0 P^\sigma)\delta(\mathbf{r}) \quad t_0 \text{ term or central term}$$
$$+ \tfrac{1}{2}t_1(1 + x_1 P^\sigma)[\mathbf{k}'^2\delta(\mathbf{r}) + \delta(\mathbf{r})\mathbf{k}^2] + t_2(1 + x_2 P^\sigma)\mathbf{k}'.\delta(\mathbf{r})\mathbf{k}$$
$$\times \ t_1, t_2 \text{ term or velocity-dependent term}$$
$$+ iW_0(\vec{\sigma}_1 + \vec{\sigma}_2) \cdot [\mathbf{k}' \times \delta(\mathbf{r})\mathbf{k}] \quad W_0 \text{ term or spin-orbit term}$$
$$+ \tfrac{1}{6}t_3(1 + x_3 P^\sigma)\rho^\alpha(\mathbf{R})\delta(\mathbf{r}) \quad \text{density-dependent term} \quad (1)$$

where $\mathbf{r} = \mathbf{r}_1 - \mathbf{r}_2$, $\mathbf{R} = \frac{1}{2}(\mathbf{r}_1 + \mathbf{r}_2)$, $\mathbf{k} = \frac{1}{2i}(\vec{\nabla}_1 - \vec{\nabla}_2)$, $\mathbf{k}'$ is the Hermitian conjugate of $\mathbf{k}$ (acting on the left), $P^\sigma = \frac{1}{2}(1 + \vec{\sigma}_1.\vec{\sigma}_2)$ is the spin-exchange operator, and ρ is the total nucleon density. The parameters $t_0, t_1, t_2, t_3, W_0, \alpha, x_0, x_1, x_2, x_3$ are obtained by fitting with experimental data [24,25].

So far, experimental data have been well reproduced without *ad hoc* adjusted parameters on nucleon elastic scattering [16] by ^{208}Pb, neutron elastic scattering [18] by ^{16}O, proton inelastic scattering [17] by ^{24}O, nucleon elastic scattering by ^{40}Ca and ^{48}Ca [19–21], and nucleon elastic scattering [22,23]
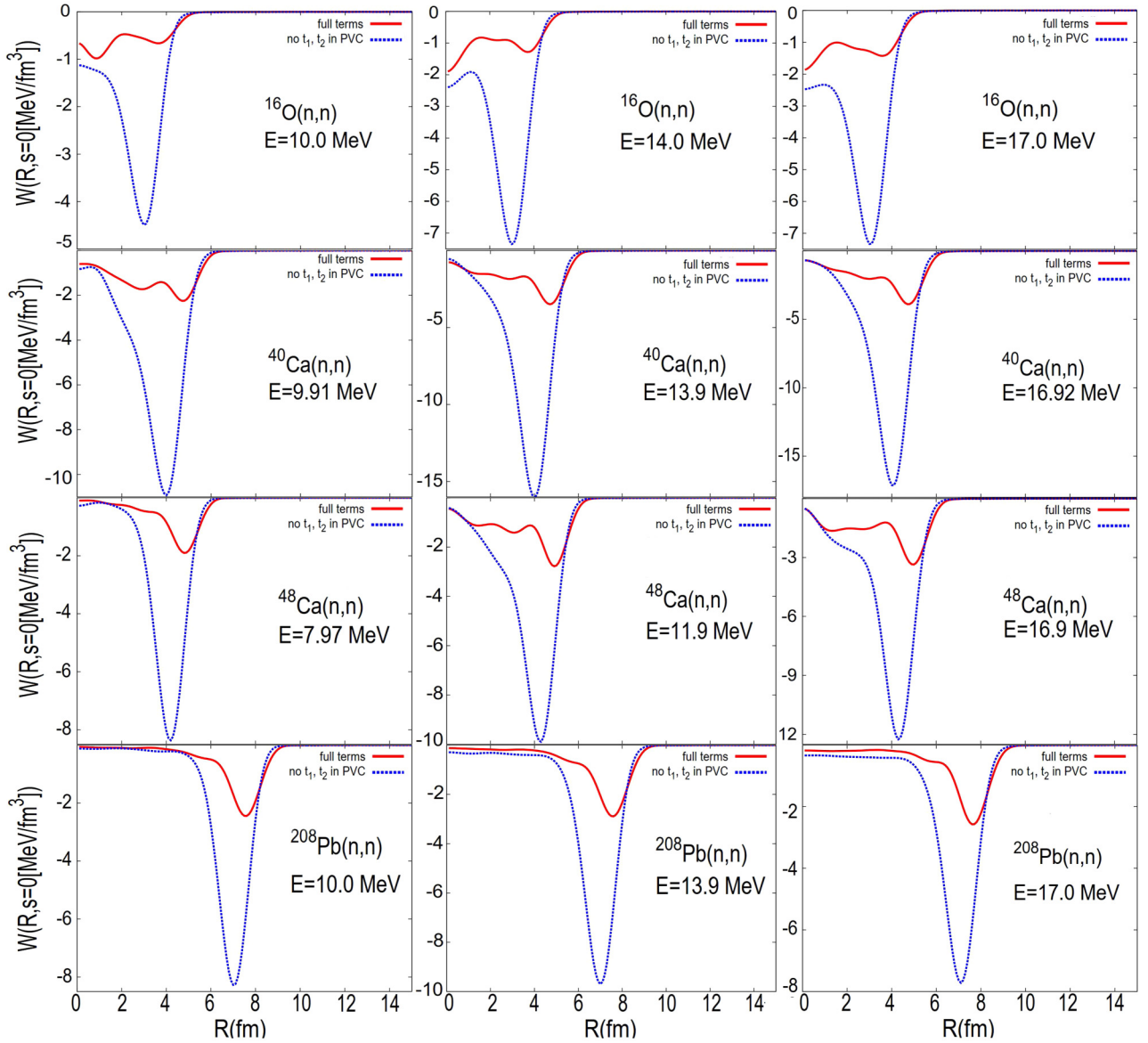
FIG. 1. The calculated $W(R, s = 0)$ for neutron elastic scattering by ^{16}O, ^{40}Ca, ^{48}Ca, and ^{208}Pb at different incident energies. The solid (dashed) curve shows the calculation with (without) t_1, t_2 terms, respectively.

by ^{16}O, ^{40}Ca, ^{48}Ca, and ^{208}Pb in the framework of the NSM (mostly with the Gogny and Skyrme interaction). However, the main drawback of these models is that the precision is not high compared with the phenomenological ones, especially the intricate deviation with experimental data at backward angles. Improvements can be done in three ways: first, in performing the NSM models; second, in refitting new variants of effective interaction which could simultaneously describe the nuclear structure and nuclear reactions; and, third, building a new generation of optical potential based on the combination of the phenomenological and microscopic approaches. In all of these ways, the effects of each term of the effective interaction on the scattering observables are very important. For example, in our work, the calculation time increases by a factor of 10 if the spin-orbit interaction is taken into account in the particle-vibration coupling (PVC). Then, for the future

applications of NSM for heavy nuclei and/or systematic calculations, we wonder whether the spin-orbit term could be neglected in order to save the calculation time.

In the pioneering work of Ref. [16], the spin-orbit, velocity-dependent, and spin-dependent terms have been dropped in the residual interaction of the PVC. Later, the two-body spin-dependent terms, the spin-orbit terms, and the Coulomb term have been neglected in the continuum RPA as well as in the continuum PVC calculations [18]. Also, due to the difficulty in the treatment of the continuum, the velocity-dependent terms have been approximately treated by the Landau-Migdal approximation. To the best of our knowledge, the only existing works of Refs. [26,27] have investigated the role of velocity-dependent and spin-orbit terms but only for nuclear structure quantities such as single-particle energies, spectroscopic factors, and the effective mass. Therefore, the
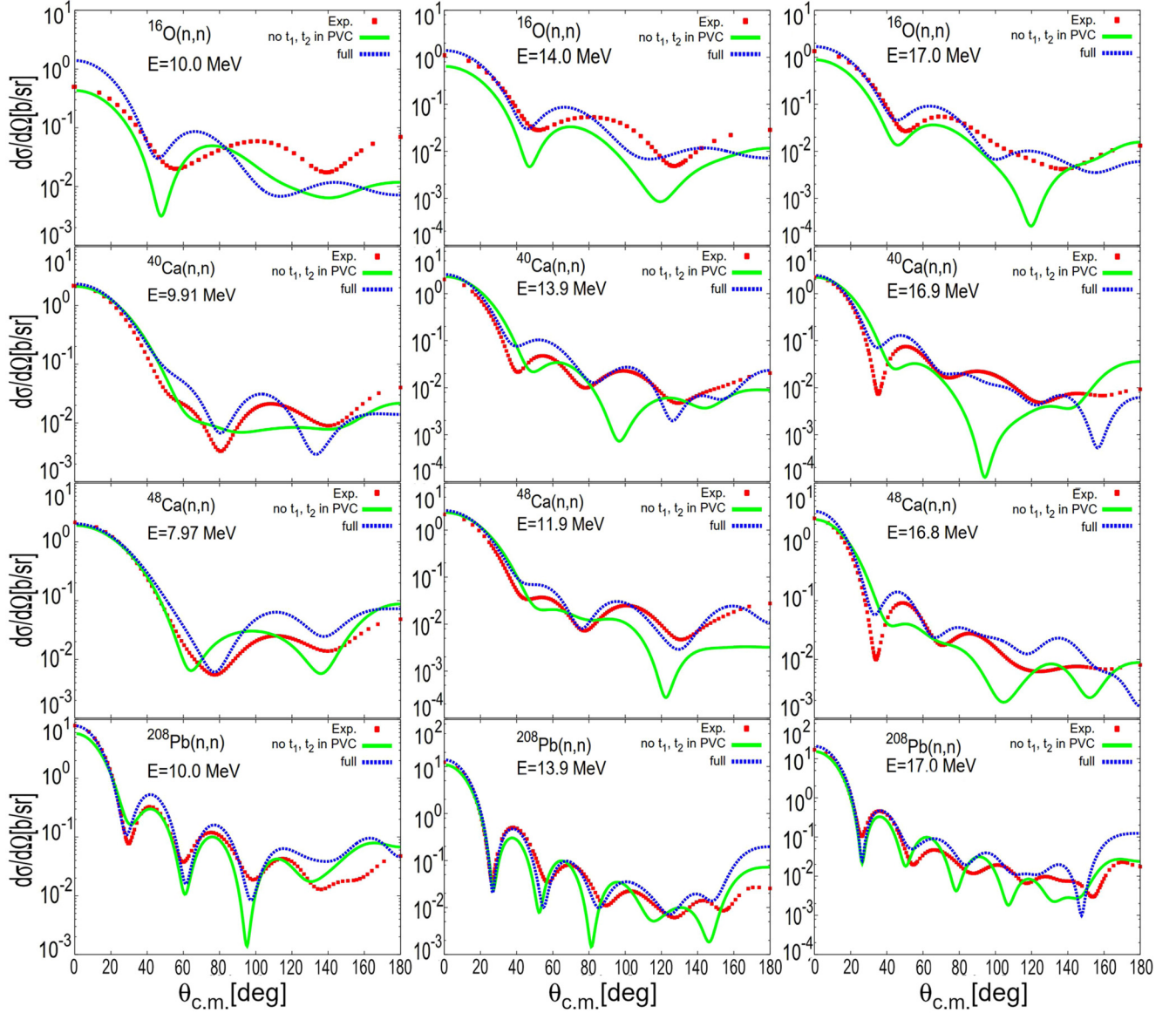
FIG. 2. Angular distributions of neutron elastic scattering by ^{16}O, ^{40}Ca, ^{48}Ca, and ^{208}Pb at different incident energies below 50 MeV. The interaction SLy5 has been used. The solid (dashed) curve shows the calculation with (without) t_1, t_2 terms, respectively. The experimental data points are taken from Ref. [33].

effects of self-consistency in using interactions on the nuclear reactions observables has never been clarified in the available literature.

As far as we know, there are two fully self-consistent calculations by G. Blanchon *et al.* [21] (with Gogny interaction) and T. V. Nhan Hao *et al.* [23] (with Skyrme interaction) where the effective phenomenological interactions have been fully and consistently used in the whole process. These calculations open the possibility to investigate the role of each term of the effective interaction.

In this paper, we will systematically investigate the effects of the velocity-dependent and spin-orbit terms on the imaginary part of the optical potential, angular distributions, and analyzing power for neutron elastic scattering off light,

medium, and heavy doubly closed shell nuclei at incident energies below 50 MeV.

II. FORMALISM

According to Refs. [22,23], the optical potential is

$$V_{\text{opt}} = V_{\text{HF}} + \Delta\Sigma(\omega), \qquad (2)$$

where

$$\Delta\Sigma(\omega) = \Sigma(\omega) - \tfrac{1}{2}\Sigma^{(2)}(\omega). \qquad (3)$$

In Eqs. (2) and (3), V_{HF} is a static Skyrme-Hartree-Fock mean field which is real, local, and energy independent. The locality arises from the zero-range character of the effective Skyrme interaction. This is one of the limits of using the
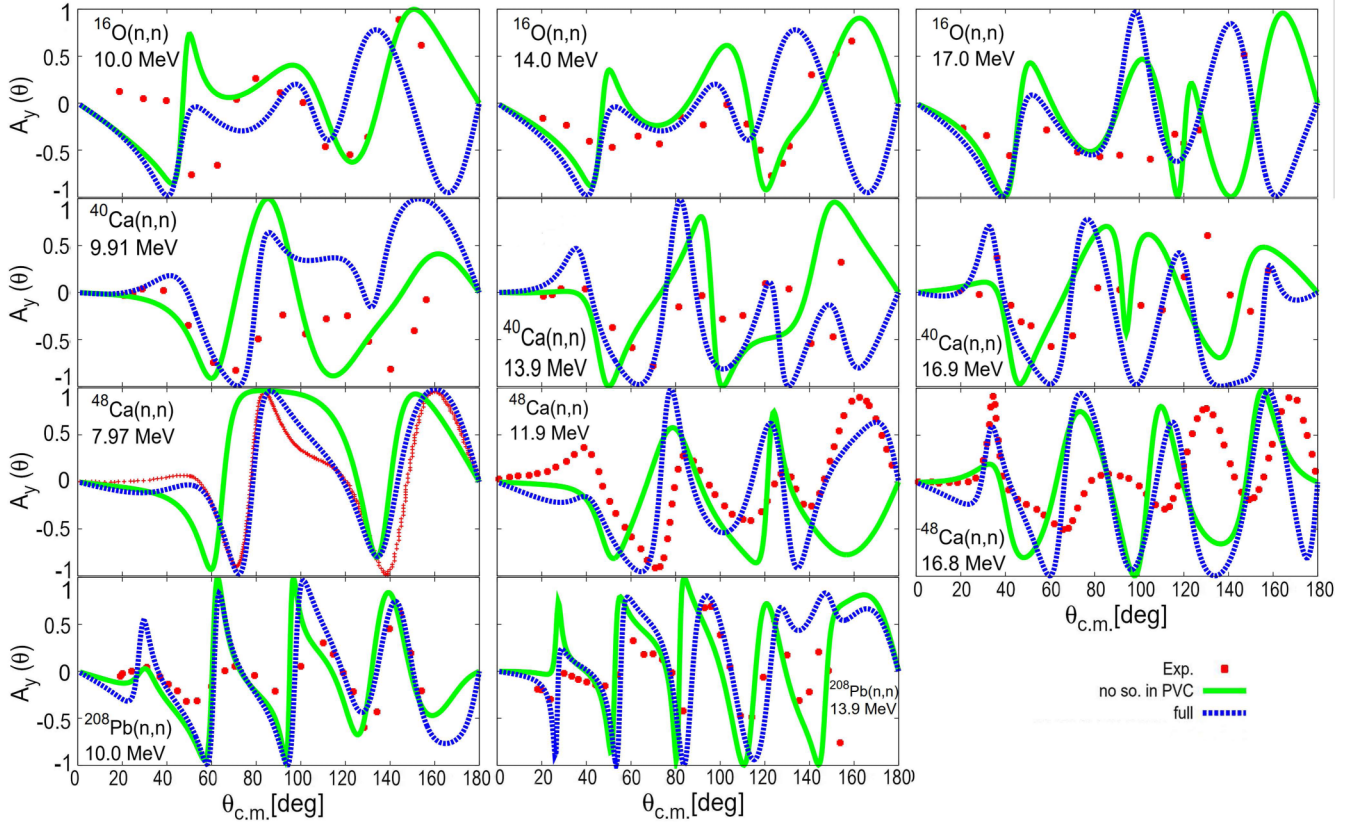
FIG. 3. Same with Fig. 2 but for analyzing power.

effective Skyrme interaction since the nonlocality plays an important role in describing this mean-field potential as in the dispersive optical potential [28,29]. This potential provides a major contribution to the real part of the optical potential. The dynamical potential, $\Delta\Sigma$, is nonlocal, complex, and energy dependent. These properties arise from channel coupling as shown in Ref. [30]. This potential gives the major contribution to the imaginary part which is responsible for the absorption of the optical potential. The real part of $\Delta\Sigma$ is small compared with the V_{HF} potential. The first-order $\Sigma(\omega)$ is the contribution from coupling to the phonon built from the particle-hole correlations. To take into account the issue of the Pauli principle correction, $\Sigma^{(2)}(\omega)$ is the second-order potential (SOP) generated from uncorrelated particle-hole contribution, and ω is the nucleon incident energy. It is worthwhile to mention that the optical potentials at the positive and negative energies are naturally and consistently connected. Then it could be useful to apply this potential to the (d,p) reaction models as the dispersive optical potential [31].

Using the partial wave expansion with the imposed spherical symmetry, the (l, j) components of $\Sigma(\omega)$ are given by

$$\Sigma_{\alpha\beta}^{(lj)}(\omega) \equiv \langle \epsilon_\alpha, lj || \Sigma(\omega) || \epsilon_\beta, lj \rangle$$

$$= \hat{j}_\alpha^{-1} \hat{j}_\beta^{-1} \left(\sum_{nL, A>F} \frac{\langle \alpha || V || A, nL \rangle \langle A, nL || V || \beta \rangle}{\omega - \epsilon_A - \omega_{nL} + i\eta} \right.$$

$$\left. + \sum_{nL, a<F} \frac{\langle \alpha || V || a, nL \rangle \langle a, nL || V || \beta \rangle}{\omega - \epsilon_a + \omega_{nL} - i\eta} \right), \quad (4)$$

where α, β are generic single-particle states, a (A) denotes the hole (particle) single-particle states, ϵ_j are the single-particle energies, ω_{nL} are the nth phonon energies with multipolarity L, $\hat{j} = (2j + 1)^{1/2}$, and the symbol F denotes the Fermi level. The parameter $\eta = 1.5$ is introduced to perform the energy averaging on the potential $\Delta\Sigma(\omega)$. The reduced matrix elements $\langle i || V || j, nL \rangle$ are the particle-vibration couplings calculated as in Refs. [23,26,27]. The residual interaction V has been fully treated and consistently used. To get the angular distributions and analyzing powers, we solve the Schrödinger equation by using the standard DWBA98 code [32] within the nonlocal, complex, and energy-dependent microscopic optical potential V_{opt}.

III. RESULTS AND DISCUSSION

We start by solving the radial HF equations in the coordinate space with the radial mesh size is 0.1 fm and the maximum value of the radial coordinate is set to be 15 fm. To describe the doubly closed-shell nuclei, the spherical symmetry has been imposed. To calculate particle states at positive energy, the continuum is discretized by imposing box boundary conditions. The NN effective phenomenological interaction SLy5 [25] has been used consistently in the whole process: mean-field, RPA, and PVC calculations. The ground states and various excited states are built on the HF solutions obtained from the fully self-consistent RPA calculations [14]. We select all the natural parity RPA excited states with the multipolarity L from 0 to 5 whose energies are smaller
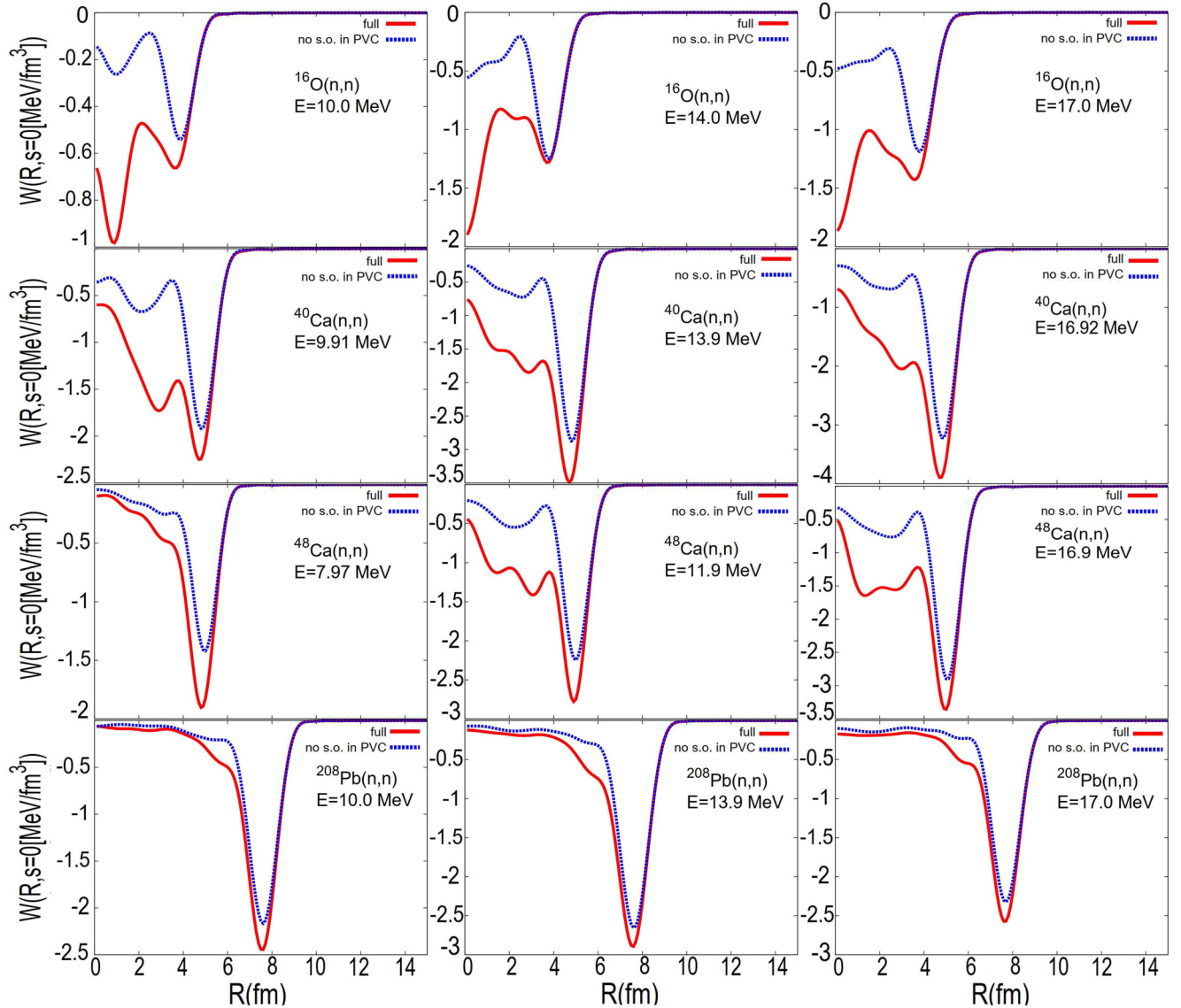
FIG. 4. The calculated $W(R, s = 0)$ for neutron elastic scattering by ^{16}O, ^{40}Ca, ^{48}Ca, and ^{208}Pb at different incident energies. The solid (dashed) curve shows the calculation with (without) spin-orbit term, respectively.

than 50 MeV and fraction of the total isoscalar or isovector strength are larger than 5% for the particle-vibration coupling calculations. The unnatural parity states have been dropped in the recent calculation. That is why, in this paper, we cannot investigate the effects of the spin-dependent terms. Note that all of these parameters are fixed for all calculated nuclei at all corresponding energies.

First, we perform two different calculations with and without t_1, t_2 terms in the residual interaction of PVC. To see the effects of these terms on the imaginary part of the optical potential, we plot the shape of diagonal contributions $W(R, s = 0)$, where $W(R, s) = \sum_{lj} \frac{2j+1}{4\pi} \mathrm{Im}\Delta\Sigma_{lj}(r, r', \omega)$, where $R = \frac{1}{2}(r + r')$ corresponds to the radius and shape of $\mathrm{Im}\Delta\Sigma$, and $s = r - r'$ shows its nonlocality. Figure 1 shows the calculations of $W(R, s = 0)$ with and without t_1, t_2 terms for neutron elastic scattering by ^{16}O, ^{40}Ca, ^{48}Ca, and ^{208}Pb at different

incident energies. It is of interest to see that, for all nuclei, the calculation with t_1, t_2 terms strongly reduce the absorption on the surface. The same effects appear in the interior region but they are much smaller. This reduction is due to the fact that the velocity-dependent part of the Skyrme force tends to reduce the coupling strength to phonons confirmed by Ref. [26]. As is well known, the velocity-dependent terms simulate somehow the finite range of Skyrme interaction in the PVC [16]. Therefore, the finite-range effects neglected in Ref. [16] (or only approximated by the Laudau-Migdal approximation in Ref. [18]) play an important role in describing the imaginary part of the optical potential, especially on the surface. To see clearly the role of t_1, t_2 terms, in Figs. 2 and 3, we systematically calculate the angular distributions and analyzing power for neutron elastic scattering by ^{16}O, ^{40}Ca, ^{48}Ca, and ^{208}Pb at different incident energies. The obtained results show that the
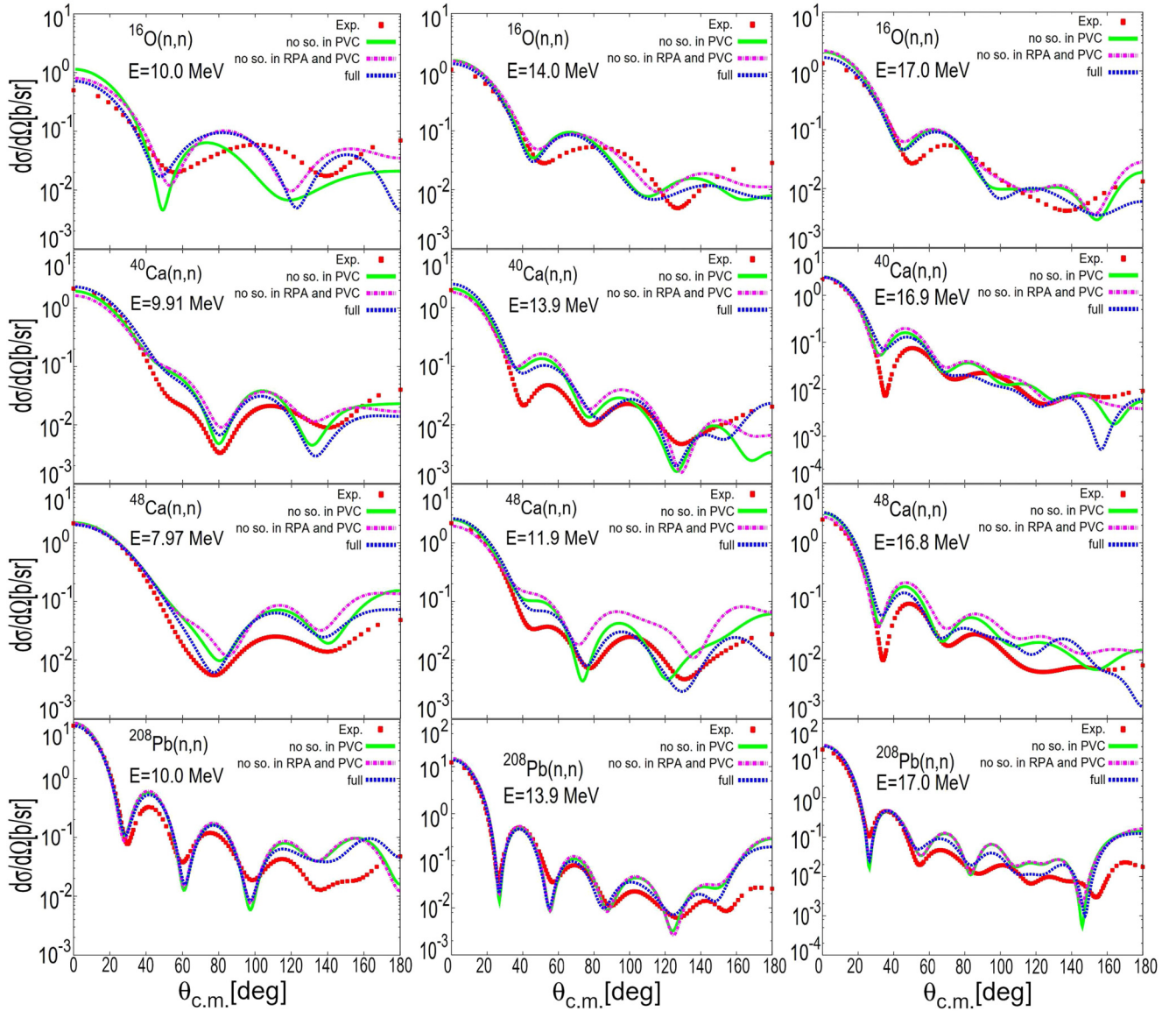
FIG. 5. Angular distributions of neutron elastic scattering by ^{16}O, ^{40}Ca, ^{48}Ca, and ^{208}Pb at different incident energies below 50 MeV. The interaction SLy5 has been used. The dotted dashed (solid) curve shows the calculation with (without) spin-orbit terms, respectively. The dashed line shows the calculation without spin-orbit term in both RPA and PVC. The experimental data points are taken from Ref. [33].

inclusion of t_1, t_2 terms strongly improves the agreement of angular distributions with experimental data. The t_1, t_2 terms do not give a systematic effect for the analyzing powers. For example, the inclusion of these terms gives a better results for ^{48}Ca at 7.97 MeV, whereas it is worse for ^{208}Pb at 10.0 MeV.

Figure 4 shows the calculations of $W(R, s = 0)$ with and without spin-orbit terms for neutron elastic scattering by ^{16}O, ^{40}Ca, ^{48}Ca, and ^{208}Pb at different incident energies. The obtained results show that the absorption strongly increases in the interior and sightly increases on the surface when the spin-orbit term is taken into account. It means that the spin-orbit part of the Skyrme interaction tends to increase the coupling strength to phonons. At the same energies and nuclei, the obtained results indicate that the effects of the velocity-dependent terms on the absorption part of the optical

potential are much stronger than ones of the spin-orbit terms. Figures 5 and 6 show the angular distributions and analyzing power for neutron elastic scattering by ^{16}O, ^{40}Ca, ^{48}Ca, and ^{208}Pb at different incident energies for there cases: with spin-orbit term in both PVC and RPA, with spin-orbit term in RPA but not in PVC, and without spin-orbit term in both PVC and RPA. For almost cases, the calculation with spin-orbit terms in both RPA and PVC gives the best angular distributions and analyzing powers compared with experimental data. Also, the inclusion of the spin-orbit term in RPA improves the agreement with experimental data. The obtained angular distributions and analyzing powers show that the effects of spin-orbit term is small in the heavy system but not negligible. Therefore, the spin-orbit term is needed even the calculation is very time-consuming.
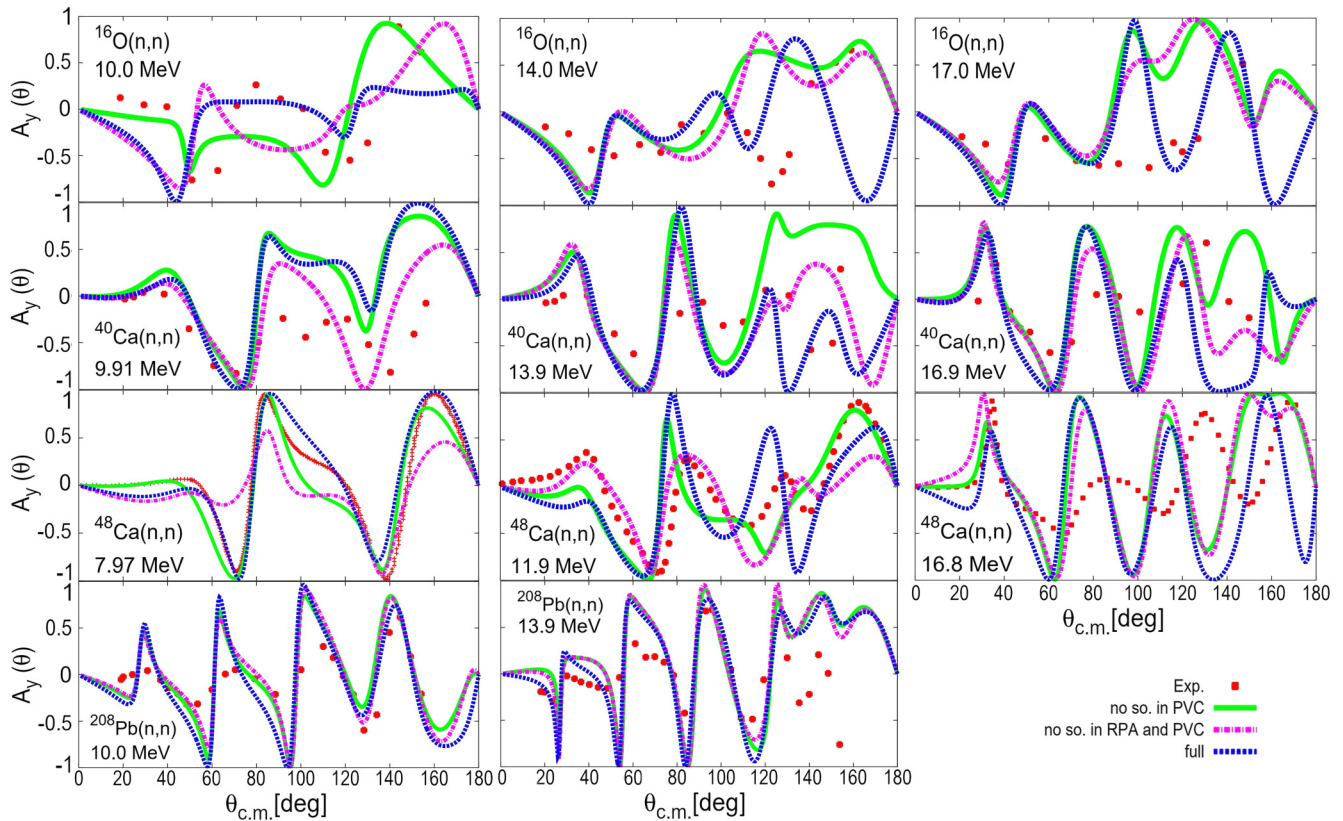
FIG. 6. Same with Fig. 5 but for analyzing power.

This work is a further step forward to develop a new generation of optical potential for the unstable nuclei region where the experimental data of the neutron elastic scattering are scarce. The obtained information will be useful to build the framework for new potentials. We propose in the near future to investigate the sensitivity of the elastic scattering observables on each parameters of the effective Skyrme interactions. Together with the obtained results in this paper, we will get enough information in the stable region before building the optical potential in the exotic nuclei region.

ACKNOWLEDGMENTS

[1] W. H. Dickhoff and R. J. Charity, Prog. Part. Nucl. Phys. **105**, 252 (2019).

[2] A. Bonaccorso, Prog. Part. Nucl. Phys. **101**, 1 (2018).

[3] A. Idini, C. Barbieri, and P. Navratil, Phys. Rev. Lett. **123**, 092501 (2019).

[4] T. R. Whitehead, Y. Lim, and J. W. Holt, Phys. Rev. C **100**, 014601 (2019).

[5] J. W. Holt, N. Kaiser, and G. A. Miller, Phys. Rev. C **93**, 064603 (2016).

[6] J. Rotureau, P. Danielewicz, G. Hagen, G. R. Jansen, and F. M. Nunes, Phys. Rev. C **98**, 044625 (2018).

[7] G. Hagen and N. Michel, Phys. Rev. C **86**, 021602(R) (2012).

[8] J. Dobaczewski, H. Flocard, and J. Treiner, Nucl. Phys. A **422**, 103 (1984).

[9] S. Fracasso and G. Colò, Phys. Rev. C **72**, 064310 (2005).

[10] P. Avogadro and C. A. Bertulani, Phys. Rev. C **88**, 044319 (2013).

[11] S. Péru and H. Goutte, Phys. Rev. C **77**, 044313 (2008).

[12] J. Terasaki, J. Engel, M. Bender, J. Dobaczewski, W. Nazarewicz, and M. Stoitsov, Phys. Rev. C **71**, 034310 (2005).

[13] J. Terasaki and J. Engel, Phys. Rev. C **82**, 034326 (2010).

[14] G. Colò, L. Cao, N. Van Giai, and L. Capelli, Comput. Phys. Commun. **184**, 142 (2013).

[15] Y. F. Niu, G. Colò, E. Vigezzi, C. L. Bai, and H. Sagawa, Phys. Rev. C **94**, 064328 (2016).

[16] V. Bernard and N. Van Giai, Nucl. Phys. A **327**, 397 (1979).

[17] K. Mizuyama and K. Ogata, Phys. Rev. C **89**, 034620 (2014).

[18] K. Mizuyama and K. Ogata, Phys. Rev. C **86**, 041603(R) (2012).

[19] G. Blanchon, M. Dupuis, R. N. Bernard, and H. F. Arellano, Eur. Phys. J. A **53**, 88 (2017).

[20] G. Blanchon, M. Dupuis, and H. F. Arellano, Eur. Phys. J. A **51**, 165 (2015).

[21] G. Blanchon, M. Dupuis, H. F. Arellano, and N. Vinh Mau, Phys. Rev. C **91**, 014612 (2015).

[22] T. V. Nhan Hao, N. Nhu Le, M. H. Koh, N. Quang Hung, N. N. Duy, V. N. T. Pham, and N. Hoang Tung, Int. J. Mod. Phys. E **27**, 1850052 (2018).

[23] T. V. Nhan Hao, B. M. Loc, and N. H. Phuc, Phys. Rev. C **92**, 014605 (2015).

[24] D. Vautherin and D. M. Brink, Phys. Rev. C **5**, 626 (1972).

[25] E. Chabanat, P. Bonche, P. Haensel, J. Meyer, and R. Schaeffer, Nucl. Phys. A **635**, 231 (1998).

[26] G. Colò, H. Sagawa, and P. F. Bortignon, Phys. Rev. C **82**, 064307 (2010).

[27] L.-G. Cao, G. Colò, H. Sagawa, and P. F. Bortignon, Phys. Rev. C **89**, 044314 (2014).

[28] W. H. Dickhoff, D. Van Neck, S. J. Waldecker, R. J. Charity, and L. G. Sobotka, Phys. Rev. C **82**, 054306 (2010).

[29] M. H. Mahzoon, R. J. Charity, W. H. Dickhoff, H. Dussan, and S. J. Waldecker, Phys. Rev. Lett. **112**, 162503 (2014).

[30] H. Feshbach, Ann. Phys. **5**, 357 (1958).

[31] N. B. Nguyen, S. J. Waldecker, F. M. Nunes, R. J. Charity, and W. H. Dickhoff, Phys. Rev. C **84**, 044611 (2011).

[32] J. Raynal, computer program DWBA98, NEA 1209/05 (1998).

[33] Experimental data taken from the National Nuclear Data Center, Brookhaven National Laboratory Online Data Service, http://www.nndc.bnl.gov/ensdf/.